JOURNAL OF COMPUTATIONAL PHYSICS 26, 352–378 (1978)

G2M, a Two-Dimensional Diffusion Time Scale Tokamak Code

R. N. BYRNE AND H. H. KLEIN

Laboratory for Applied Plasma Studies, Science Applications, Inc., La Jolla, California 92037

Received September 1, 1976; revised June 16, 1977

The equations describing the diffusion time scale evolution of a tokamak separate into two types, a 2D elliptic equation and a set of 1D parabolic equations. The equations are coupled in that the 1D set provides the inhomogeneous source for the 2D equation, while the 2D equation provides both the source and the geometry for the 1D set. The G2M code solves these equations on a moving orthogonal coordinate system with the grid lines tied to magnetic flux, as a Lagrangian formulation of fluid mechanics ties the grid to the fluid. The techniques required to do this are described, and examples of code runs are presented.

I. INTRODUCTION

The energy crisis has sharpened the longstanding interest in fusion reactors. Such reactors would "burn" hydrogen isotopes rather than fission uranium as do present nuclear reactors, and would be a way to produce nuclear power without generating fission products. The advantages of fusion power are discussed in a recent review article by Ribe [1].

One of the most interesting of the many devices proposed as possible fusion reactors is the tokamak, a toroidal machine with a current-carrying hot plasma. The concept is described by Artsimovich [2], the U. S. tokamak effort is reviewed by Dean *et al.* [3], and recent developments are covered by Furth [4]. Briefly, the idea is to take advantage of the fact that the ionized hydrogen tends to resist diffusion of mass and heat across a strong magnetic field. This field can be produced by an electric current flowing in the plasma itself. There are no end losses, because of the toroidal geometry. A strong toroidal magnetic field, produced by current windings outside the plasma, renders the plasma magnetohydrodynamically stable.

The ideal field configuration is that of a family of nested magnetic surfaces, field lines spiraling around the torus but always remaining on a particular toroidal surface. These are referred to as flux surfaces. Other field geometries (magnetic islands, for example) are conceivable but we will restrict ourselves to consideration of this topology. Figure 1 illustrates the field helices and Fig. 2 illustrates flux surfaces.

Transport of heat or mass in a plasma is much easier along a strong magnetic field line than across it. For irrational pitch of the magnetic helices any point on a flux surface can be approached arbitrarily closely in a finite distance by traveling along a

0021-9991/78/0263-0352$02.00/0

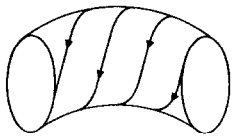

FIG. 1. Magnetic field helices around a section of the torus.

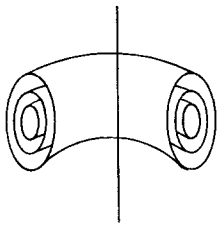

Fig. 2. Nested flux surfaces.

field line starting from any other point on the surface. Therefore density and temperature variations are expected to be less in a flux surface than across flux surfaces, an interesting feature of this geometry. We may ignore toroidal variation because of the symmetry of the device, but it is the physics that will allow us to ignore variation of density and temperature in the flux surface.

Chu et al [5] discuss the numerical difficulties caused by the enormous anisotropy of heat diffusion in a magnetized plasma. These difficulties are obviated by the use of flux surfaces as coordinates. This and the constancy of density and temperature on these surfaces have led us to adopt flux surface coordinates.

Another feature of the machine is the large separation of time scales. Grad and Hogan [6] discuss in particular the diffusion time scale with which we shall be concerned. On this time scale the fast magneto-hydrodynamic (MHD) activity has died away, the configuration being assumed MHD stable. The plasma and field are then in equilibrium. This determines the shapes and positions of the flux surfaces. These can still change as the determining parameters evolve. This evolution is assumed to proceed on a considerably slower time scale than that describing MHD activity. Diffusion resulting from collisions can produce such changes.

The laws of conservation of magnetic flux, mass and energy, coupled with a transport theory of diffusion, give a complete description of the evolution of current, density, and temperature. This description can be reduced to a one-dimensional (1D) one, since the relevant parameters change only across flux surfaces. A knowledge of the shapes of the flux surfaces is required for the solution of the resulting equations. Although it is not strictly consistent to do so, it is possible to assume this knowledge a priori. Many 1D codes have been written using essentially this model (for a review, see Hogan's article [7]).

In fact the shapes are determined by the solution of this 1D problem, supplemented by boundary conditions and the statement of force balance in the plasma. Therefore a consistent calculation is possible, with the shapes changing in response to diffusion

and the diffusion being influenced by the instantaneous shapes. A two-dimensional (2D) calculation is thus required, shapes being inherently 2D. This was pointed out by Grad [8], Hinton and Hazeltine [9], and others, and forms the basis of the G2M code described herein. Other codes based on this principal have been reported by Helton, Miller, and Rawls [10] at General Atomic, Todd and Grimm [11] at Princeton Plasma Physics Laboratory, and Gardner and Boris [12] at the Naval Research Laboratory.

Although the mathematical structure of a tokamak code is imposed by the problem, the details of the transport process are still not completely worked out. The current status of tokamak transport theory is reviewed by Hinton and Hazeltine [9]. These authors [13] have presented an elegant solution for the flux surface averaged transport, valid in the "collisional" Pfirsch-Schlüter regime. We have used their results in G2M, since they are for general geometry, and since this regime is accessible to experiment using existing machines.

With the restriction to Pfirsch-Schlüter transport the problem is completely stated.[1] The remainder of this paper discusses the above ideas in more detail and demonstrates a technique for solving the problem on a computer, concluding with some examples of the sort of problems that can now be solved.

II. Definitions and Basic Equations

We consider a plasma composed of electrons and ions. The electrons have density n_e, temperature T_e, and pressure $P_e = n_e k T_e$, where k is Boltzman's constant. Similarly, the ions are described by n_i, T_i, and P_i. The ions are a mixture of various atomic species such that the average charge is $\bar{z}$. This and the average square charge, $\bar{z}^2$, are constant in space and time.

There is a flux of electrons, $\boldsymbol{\Gamma}_e$; the corresponding flux of ions maintains charge neutrality. Ionizations provide a source S of electrons. Heat is conducted by the electrons and ions, the fluxes being $\mathbf{Q}_e$ and $\mathbf{Q}_i$. The two species exchange energy at the rate Q_Δ. The electric field $\mathbf{E}$ delivers energy to the plasma at the rate $\mathbf{j} \cdot \mathbf{E}$, where $\mathbf{j}$ is the current. H_i of this power goes directly to the ions, the rest goes to the electrons. R_e and R_i denote all other local energy gains or losses, due for instance to line radiation, charge exchange, ionization, or auxiliary heating devices.

These quantities are related by conservation laws. The statement of electron conservation is

$$\frac{\partial n_e}{\partial t} + \nabla \cdot \boldsymbol{\Gamma}_e = S \tag{1}$$

Charge neutrality gives the ion density

$$n_i = \frac{n_e}{\bar{z}} \tag{2}$$

[1] The reader is referred to a recent paper [14] of Pao for an alternative view of the problem.

Electron energy is $\frac{3}{2}P_e$. Its conservation law is

$$\frac{3}{2}\frac{\partial P_e}{\partial t} + \nabla \cdot \left(\mathbf{Q}_e + \frac{5}{2}kT_e\boldsymbol{\Gamma}_e\right) = \mathbf{j}\cdot\mathbf{E} - H_i - Q_\Delta + R_e \tag{3}$$

For ions we have

$$\frac{3}{2}\frac{\partial P_i}{\partial t} + \nabla \cdot \left(\mathbf{Q}_i + \frac{5}{2}kT_i\frac{\boldsymbol{\Gamma}_e}{\bar{z}}\right) = H_i + Q_\Delta + R_i \tag{4}$$

The plasma is permeated by a magnetic field **B**, related to the current by Ampere's law

$$\nabla \times \mathbf{B} = \frac{4\pi}{c}\mathbf{j} \tag{5}$$

Conservation of magnetic flux is expressed by Faraday's law

$$\frac{\partial \mathbf{B}}{\partial t} = -c\nabla \times \mathbf{E} \tag{6}$$

On the long time scale with which we shall be concerned the system passes through a succession of equilibria as plasma and field slowly diffuse. This implies that current, field and total pressure, $P = P_e + P_i$, are related by the law of force balance

$$\mathbf{j} \times \mathbf{B} = c\nabla P \tag{7}$$

It is advantageous to use cylindrical (r, φ, Z) coordinates, because of the toroidal symmetry of tokamaks. The toroidal angle φ is therefore ignorable $(\partial/\partial\varphi = 0)$. Further simplification results from expressing **B** in terms of the two scalar variables f and ψ, where $f = r\mathbf{B}_\varphi$ and ψ is the poloidal flux. That is,

$$\mathbf{B} = f\nabla\varphi + \nabla\varphi \times \nabla\psi \tag{8}$$

This form automatically satisfies

$$\nabla \cdot \mathbf{B} = 0 \tag{9}$$

Faraday's law, Eq. (6), relates $\dot{\psi}$ to $\mathbf{E}_\varphi$, to within a constant of integration, which we choose to be zero:

$$\dot{\psi} = rc\mathbf{E}_\varphi \tag{10}$$

Flux surfaces are surfaces of constant ψ. Since magnetic field lines lie in flux surfaces and since many of the variables of interest are constant on flux surfaces, it is convenient to use a coordinate system having ψ as a coordinate. We choose φ as a second coordinate, because of the toroidal symmetry. χ, the poloidal coordinate, is chosen mutually orthogonal to ψ and φ. The coordinate systems used are illustrated in Fig. 3.

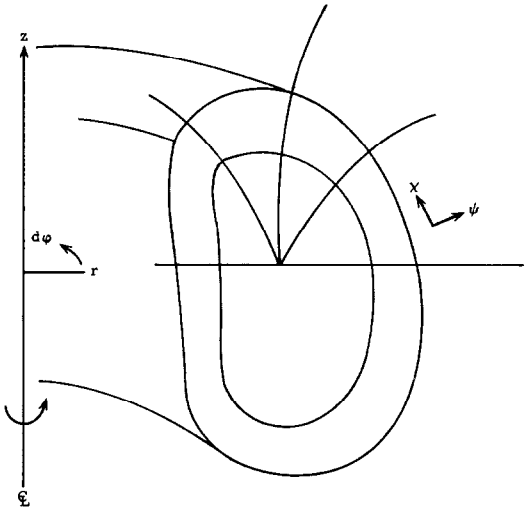

FIG. 3. Coordinate systems.

III. EQUATIONS TO BE SOLVED

Force balance, Eq. (7), together with Ampere's law Eq. (5), imply that P and f are constant on a flux surface. They also imply

$$\nabla \cdot \frac{1}{r^2} \nabla\psi + 4\pi \frac{\partial P}{\partial \psi} + \frac{1}{r^2} f \frac{\partial f}{\partial \psi} = 0 \tag{11}$$

Equation (11) is referred to as the Grad-Shafranov equation [15, 16]. It will be the single 2D equation the code must solve.

The particle and energy conservation laws, Eqs. (1), (3), and (4), are basically one-dimensional. To see why, note that variation of the temperatures is small along the field lines because of the large heat conductivity along the magnetic field lines. We have taken n_e to be a constant multiple of n_i, so the constancy of total pressure then implies that the particle densities are also constant on a flux surface. To this approximation, then, P_e and P_i are separately constant on a flux surface.

We wish to extract a set of equations that explicitly displays this one-dimensionality. First, rewrite the equations in the (ψ, φ, χ) coordinate frame, which moves because ψ changes with time according to Eq. (10). Second, eliminate references to χ by averaging the equations over a small volume surrounding a flux surface. These two steps require the introduction of some new quantities. We shall discuss these before presenting the resulting 1D equations.

Time derivatives in this frame will be denoted by D/Dt, thus

$$\frac{D\psi}{Dt} = 0 \tag{12}$$

expresses the fact that this frame moves such that ψ remains constant on a grid line. If $\mathbf{v}_G$ is the velocity of the grid,

$$\dot{\psi} + \mathbf{v}_G \cdot \nabla\psi = 0 \tag{13}$$

Equations (8), (10) and (13) then imply

$$(\mathbf{v}_G)_\psi = c\,\frac{\mathbf{E}_\varphi}{\mathbf{B}_x} \tag{14}$$

Thus there is no toroidal electric field in the frame that moves with the grid:

$$\left(\mathbf{E} + \frac{\mathbf{v}_G \times \mathbf{B}}{c}\right)_\varphi = 0 \tag{15}$$

The electron flux relative to this grid is due solely to collisions and will be denoted $\mathbf{\Gamma}_c$. It satisfies

$$\mathbf{\Gamma}_c = \mathbf{\Gamma} - n_e\mathbf{v}_G \tag{16}$$

The grid velocity also enters the expression for the power delivered by the fields:

$$\mathbf{j} \cdot \mathbf{E} = -\frac{c}{4\pi}\frac{\partial f}{\partial \psi}\,\mathbf{E} \cdot \mathbf{B} + \mathbf{v}_G \cdot \nabla P \tag{17}$$

We assign $\mathbf{v}_G \cdot \nabla P_i$ of this power to the ions, the rest to the electrons, so

$$H_i = \mathbf{v}_G \cdot \nabla P_i \tag{18}$$

This expression for $\mathbf{j} \cdot \mathbf{E}$ is consistent with that of Hinton and Hazeltine [9] and may be derived from Ampere's law, Eq. (5), force balance, Eq. (7), and the definition of $\mathbf{v}_G$.

Finally we define the volume average of a quantity over a surface. Let $V(\psi, t)$ be the volume contained within a ψ surface per radian of toroidal angle. We shall sometimes denote ψ derivatives by primes, in particular: $V' \equiv \partial V/\partial\psi$. The flux surface average of a quantity A is defined by

$$\langle A \rangle = \frac{\partial}{\partial V}\int_V A\, d^3x \tag{19}$$

where the integral is over the volume contained within a flux surface. This average has the property that $\langle \mathbf{B} \cdot \nabla A \rangle = 0$ for any A. Using Gauss' theorem one can show

$$\langle \nabla \cdot \mathbf{A} \rangle = \frac{\partial}{\partial V}\langle \mathbf{A} \cdot \nabla V \rangle \tag{20}$$

for any vector **A**.

Using the above definitions, we average the conservation laws, Eqs. (1), (3) and (4), over the moving ψ surfaces to find the desired one dimensional set of conservation laws:[2]

$$\frac{DnV'}{Dt} + \frac{\partial}{\partial\psi}\langle \Gamma_e \cdot \nabla V\rangle = \langle S\rangle V' \tag{21}$$

$$\frac{3}{2}\frac{DP_eV'}{Dt} + P_e\frac{DV'}{Dt} + \frac{\partial}{\partial\psi}\left\langle\left(\mathbf{Q}_e + \frac{5}{2}kT_e\Gamma_e\right)\cdot\nabla V\right\rangle$$

$$= \left(-\frac{c}{4\pi}f'\langle \mathbf{E}\cdot\mathbf{B}\rangle - Q_\Delta + \langle R_e\rangle\right)V' \tag{22}$$

$$\frac{3}{2}\frac{DP_iV'}{Dt} + P_i\frac{DV}{Dt} + \frac{\partial}{\partial\psi}\left\langle\left(\mathbf{Q}_i + \frac{5}{2}kT_i\Gamma_c/\bar{z}\right)\cdot\nabla V\right\rangle = (Q_\Delta + \langle R_i\rangle)V' \tag{23}$$

A similar treatment of the toroidal component of Faraday's law, Eq. (6), expresses conservation of toroidal flux:

$$\frac{D\left(f\left\langle\frac{1}{r^2}\right\rangle V'\right)}{Dt} + \frac{\partial}{\partial\psi}V'\langle c\mathbf{E}\cdot\mathbf{B}\rangle = 0 \tag{24}$$

The quantity in parenthesis in the above equation, divided by 2π, is known as the safety factor q. It measures the number of toroidal circuits a field line takes per poloidal circuit.

As we shall see, Γ_c, the Q's, and $\mathbf{E}\cdot\mathbf{B}$ are due to collisions. In their absence, Eqs. (21)–(24) reduce to the adiabatic set

$$\frac{DnV'}{Dt} = 0 \tag{25}$$

$$\frac{3}{2}\frac{DP_eV'}{Dt} + P_e\frac{DV'}{Dt} = 0 \tag{26}$$

$$\frac{3}{2}\frac{DP_iV'}{Dt} + P_i\frac{DV'}{Dt} = 0 \tag{27}$$

$$\frac{Dq}{Dt} = 0 \tag{28}$$

This clearly displays the effect of adiabatic compression, namely that particles, entropy, and safety factor are all conserved.

Hazeltine and Hinton [13] quote specific results for the fluxes needed, in the Pfirsch-Schlüter regime. Let c = speed of light, e = electron charge m = electron

[2] See Appendix A for details of the derivation.

mass, M = ion mass, τ = electron-ion collision time, τ_i = ion-ion collision time. λ_{ij} are numerical factors depending on the ratio $\bar{z}^2/\bar{z}$.

$$\langle \Gamma_c \cdot \nabla V \rangle = V' \left(\left\langle \frac{1}{B^2} \right\rangle - \frac{1}{\langle B^2 \rangle} \right) \left(- \frac{f^2 c^2 m}{e^2 \tau} \right) \left(\frac{\lambda_{22}}{\lambda} P' - \frac{5}{2} \frac{\lambda_{12}}{\lambda} n_e k T_e' \right) + V' f c n_e \frac{\langle \mathbf{E} \cdot \mathbf{B} \rangle}{\langle B^2 \rangle} \tag{29}$$

$$\langle \mathbf{Q}_e \cdot \nabla V \rangle = V' \left(\left\langle \frac{1}{B^2} \right\rangle - \frac{1}{\langle B^2 \rangle} \right) \left(- \frac{f^2 c^2 m}{e^2 \tau} k T_e \right) \left(\frac{25}{4} \frac{\lambda_{11}}{\lambda} n_e k T_e' - \frac{5}{2} \frac{\lambda_{12}}{\lambda} P' \right) \tag{30}$$

$$\langle \mathbf{Q}_i \cdot \nabla V \rangle = V' \left(\left\langle \frac{1}{B^2} \right\rangle - \frac{1}{\langle B^2 \rangle} \right) \left(-1.6 \frac{f^2 c^2 M}{e^2 \tau_i} \right) P_i k T_i' \tag{31}$$

The generally smaller classical transport terms have been neglected in Eqs. (29)-(31).

The electron-ion heat exchange is the classical value [17, 18]

$$Q_\Delta = \frac{3Mk}{m} \frac{n_e}{\tau} (T_e - T_i) \tag{32}$$

The electron energy conservation equation (22) and the flux conservation equation (24), require a knowledge of $\langle \mathbf{E} \cdot \mathbf{B} \rangle$. We use an Ohm's law of the form [18]

$$\mathbf{E} + \frac{\mathbf{V} \times \mathbf{B}}{c} + \frac{\nabla P_e}{e n_e} = \eta \cdot \mathbf{j} + \frac{\mathbf{j} \times \mathbf{B}}{e n_e c} - \frac{\lambda \mathbf{B} (\mathbf{B} \cdot \nabla k T_e)}{e B^2} - \frac{3}{2} \frac{1}{e \omega \tau} \frac{\mathbf{B} \times \nabla k T_e}{|\mathbf{B}|} \tag{33}$$

where λ is a function of the ionic charge, ω is the electron cyclotron frequency, and η is the resistivity tensor. The use of this form of Ohm's law is consistent with the calculation by Hazeltine and Hinton [13] of transport coefficients in the Pfirsch-Schlüter regime.

This gives

$$\langle \mathbf{E} \cdot \mathbf{B} \rangle = \eta_\parallel \langle \mathbf{j} \cdot \mathbf{B} \rangle \tag{34}$$

where $\eta_\parallel$ is the parallel component of the resistivity tensor.

Notice that Eqs. (21) — (24) contain no advective terms, i.e., no first derivatives (in ψ) of the quantities of interest n, P_e, P_i, or f. The presence of such terms can lead to artificially enhanced diffusion in numerical solutions to the conservation laws. The use of a moving grid to eliminate these terms is reminiscent of the use of Lagrangian grids in fluid mechanics.

The calculation of $\mathbf{j} \cdot \mathbf{B}$ will be performed in the (ψ, φ, χ) coordinate system. The components of the current can be obtained from Ampere's law, Eq. (5):

$$\mathbf{j}_\varphi = \frac{cr}{4\pi} \nabla \cdot \frac{1}{r^2} \nabla\psi \tag{35}$$

$$\mathbf{j}_\chi = \frac{-c}{4\pi} f' \mathbf{B}_\chi \tag{36}$$

$$\mathbf{j}_\psi = 0 \tag{37}$$

The components of the magnetic field can be obtained from Eq. (8).

$$\mathbf{B}_\varphi = \frac{f}{r} \tag{38}$$

$$\mathbf{B}_\chi = \frac{-|\nabla\psi|}{r} \tag{39}$$

$$\mathbf{B}_\psi = 0 \tag{40}$$

It will be useful to introduce Grad's K function [19]. K is defined by

$$K(V) = \left\langle \left(\frac{\nabla V}{r} \right)^2 \right\rangle \tag{41}$$

Note that K depends only on the shapes of the flux surfaces enclosing volume V and not upon the physical variables. We find

$$\langle \mathbf{j} \cdot \mathbf{B} \rangle = \langle \mathbf{j}_\varphi \mathbf{B}_\varphi \rangle + \langle \mathbf{j}_\chi \mathbf{B}_\chi \rangle = \frac{c}{4\pi} f \left\langle \nabla \cdot \frac{1}{r^2} \nabla\psi \right\rangle - \frac{c}{4\pi} f' \langle \mathbf{B}_\chi^2 \rangle \tag{42}$$

Using Gauss' law, equation (20), and the definition of K, Eq. (41)

$$\langle \mathbf{j} \cdot \mathbf{B} \rangle = \frac{c}{4\pi} f^2 \frac{\partial}{\partial V} \left(\frac{1}{f} \frac{K}{V'} \right) \tag{43}$$

An alternate expression for $\langle \mathbf{j} \cdot \mathbf{B} \rangle$ follows from replacing $\nabla \cdot (1/r^2) \nabla\psi$ in equation (42) with its value as determined by the Grad-Shafranov equation, (11):

$$\langle \mathbf{j} \cdot \mathbf{B} \rangle = -cfP' - \frac{c}{4\pi} f^2 f' \left\langle \frac{B^2}{\mathbf{B}_\varphi^2} \frac{1}{r^2} \right\rangle \tag{44}$$

We find a useful form of the flux surface averaged toroidal current by applying Gauss' law to equation (35):

$$\left\langle \frac{4\pi}{rc} \mathbf{j}_\varphi \right\rangle = \frac{\partial \left(\frac{K}{V'} \right)}{\partial V} \tag{45}$$

This form shows that K/V' is the toroidal current contained within the flux surface of volume V, times $4\pi/c$.

In conventional tokamaks the plasma does not appreciably affect the field, so in the code $\mathbf{B}_x^2$ is neglected with respect to B_φ^2, and Eqs. (43) and (44) become

$$\langle \mathbf{j} \cdot \mathbf{B} \rangle = f \frac{\partial}{\partial V} \left(\frac{K}{V'} \right) \tag{43a}$$

$$\langle \mathbf{j} \cdot \mathbf{B} \rangle = -cfP' - \frac{c}{4\pi} f^2 f' \left\langle \frac{1}{r^2} \right\rangle \tag{44a}$$

This completes the set of differential equations to be solved on the computer. The fundamental ones are Eqs. (21)-(24). We should like to emphasize that the form of these equations is quite general, being based on conservation laws and on the assumption that n, T_e, and T_i can be replaced by their flux surface averages. The form of the transport terms $\mathbf{Q}$, ∇, etc., would of course be different if different physical processes (e.g., turbulence) were considered.

IV. Boundary Conditions

The 1D equations, (21)-(24), require for consistency the internal boundary condition that n_e, P_e, P_i, and f remain finite at the magnetic axis, $V = 0$. Their values, or the fluxes Γ, $\mathbf{Q}$, $\langle E \cdot B \rangle$, will be specified as functions of time on the outer boundary.

The fluxes given by Eqs. (29) and (34) do not vanish at the axis. This is because these fluxes are with respect to a moving flux surface. The magnetic axis, however, is not a surface of constant ψ. The appropriate fluxes there are those with respect to a fixed surface. The particle flux is then [cf Eq. (16)]:

$$\langle \mathbf{\Gamma} \cdot \nabla V \rangle = \langle \mathbf{\Gamma}_c \cdot \nabla V \rangle + n_e \langle \mathbf{v}_G \cdot \nabla V \rangle \tag{46a}$$

$$= \langle \mathbf{\Gamma}_c \cdot \nabla V \rangle + n_e c V' \left\langle \frac{\mathbf{E}_\varphi}{\mathbf{B}_x} \mid \nabla \psi \mid \right\rangle \tag{46b}$$

$$= \langle \mathbf{\Gamma}_c \cdot \nabla V \rangle - n_e c V' f \left\langle \frac{\mathbf{E}_\varphi}{\mathbf{B}_\varphi} \right\rangle \tag{46c}$$

At the axis $\mathbf{E}_x$ and $\mathbf{B}_x$ vanish, so upon substituting for $\mathbf{\Gamma}_c$ from Eq. (29) one finds that the particle flux is in fact zero on the axis.

The heat fluxes, given by Eqs. (30) and (31), are independent of the reference frame, and hence valid on the axis in that form. They also are seen to vanish there.

The flux of safety factor given by Eq. (34) does depend on the reference frame. Faraday's law for a fixed grid requires the integral of $\mathbf{E}_x \mathbf{B}_x$, not $\mathbf{E} \cdot \mathbf{B}$. Clearly $\mathbf{E}_x \mathbf{B}_x$ vanishes on the axis.

Specification of ψ on a closed surface W containing the plasma is a sufficient

boundary condition for the solution of the Grad-Shafranov equation, (11). Equation (10) shows that specification of $\psi_w(t)$ is equivalent to specifying the loop voltage applied. Because Eq. (11) is to be solved simultaneously with the 1D set, Eqs. (21)-(24), the total current contained in the system depends on this applied voltage.

Experience has shown that it is preferable to specify the total current carried by the plasma rather than the voltage applied. This is in accord with the results of the simple model

$$\frac{dT}{dt} = \frac{-T}{T^{\frac{3}{2}}} + VI \tag{47}$$

$$I = T^{\frac{3}{2}}V \tag{48}$$

The resulting temperature T is stable to perturbations if the current I is fixed, and unstable if the voltage V is fixed.

Therefore, for boundary conditions on the system, we fix the location of the outermost flux surface and specify the total current $I(t)$. ψ_w is determined parametrically.

V. Numerical Scheme

We have seen that the essential features of a tokamak, on the long time scale, are represented by a set of four parabolic 1D equations, to be solved simultaneously with an elliptic 2D equation.

In this section we discuss: first the numerical method used to solve the 2D Grad-Shafranov equation, second the methods used to solve the 1D equations, and third the method used to solve both self-consistently.

The Grad-Shafranov equation, (11), determines ψ given the functions $P(\psi)$ and $f(\psi)$. The scheme used to solve this equation is an iterative one suggested by Potter and Tuttle [20, 21]. An (i, j) grid is defined: the j lines are to be contours ψ_j = constant. A contour grid is inherently more accurate than a rectangular grid because a rectangular grid must resolve gradients skewed to the mesh, and because the contour grid concentrates in regions of large gradients. Therefore, the number of grid lines required for a given accuracy is less on a contour grid; one has resolution where needed without paying the price of fine spacing everywhere.

The problem has been converted into one of finding the position of the contours, as in Lagrangian hydrodynamics, although here the location of the i lines is arbitrary.

The spatial derivatives of the Grad-Shafranov equation contain mixed i, j derivatives in general. These vanish if the i lines are chosen orthogonal to the j lines (ψ contours), and the resulting form suggests simple difference approximations that can be solved by standard techniques, such as ADI. We therefore use Potter and Tuttle's elegant orthogonalization technique [22] to define the lines of i. The coordinate system is thus (j, φ, i), where i and j play the roles of the χ and ψ coordinates of Fig. 3.

The iterative process begins with an assumed location of the j lines. The functions $P'(\psi)$ and $ff'(\psi)$ are replaced by $P_j' = P'(\psi_j)$ and ff_j'. We of course know r_{ij}, the

radial position of the grid points. Under these assumptions we know the current $\mathbf{j}_\varphi$ at every grid point:

$$\frac{4\pi}{r_{ij}c}(\mathbf{j}_\varphi)_{ij} = -4\pi P_j' - (ff')_j \frac{1}{r_{ij}^2} \tag{49}$$

We now solve

$$\nabla \cdot \frac{1}{r^2} \nabla\psi = \frac{4\pi}{rc} \mathbf{j}_\varphi \tag{50}$$

As mentioned previously, the operator is diagonal in this coordinate system. Let h_i, h_j be the metric functions on the grid, so that $h_i di$ is the distance separating two points on a j line at (i) and $(i + di)$. Then (49) and (50) become

$$\frac{1}{rh_ih_j}\left[\frac{\partial}{\partial i}\frac{h_j}{rh_i}\frac{\partial\psi}{\partial i} + \frac{\partial}{\partial j}\frac{h_i}{rh_j}\frac{\partial\psi}{\partial j}\right] + 4\pi P_j + \frac{ff_j'}{r_{ij}^2} = 0 \tag{51}$$

The result of differencing this equation is a matrix equation

$$H\psi + V\psi + S = 0 \tag{52}$$

where H is the matrix that connects $\psi(i,j)$ with $\psi(i \pm 1, j)$, V connects $\psi(i,j)$ with $\psi(i, j \pm 1)$, and S is everything else. This matrix equation may be solved exactly, for example by Gaussian elimination. However, we choose the ADI technique [23]. We introduce an iteration scheme producing a series of approximate solutions ψ^i. A damping factor D is needed for convergence; the final answer does not depend on D.

Let ψ^* solve the one-dimensional set of equations

$$H\psi^i + V\psi^* + S + D(\psi^* - \psi^i) = 0 \tag{53}$$

Then let ψ^{**} solve the one-dimensional set of equations

$$H\psi^{**} + V\psi^* + S + D(\psi^{**} - \psi^*) = 0 \tag{54}$$

and let

$$\psi^{i+1} = \frac{\psi^{**} + \psi^i}{2} \tag{55}$$

Manipulation gives

$$H\psi^{i+1} + V\psi^{i+1} + S = -E(\psi^{i+1} - \psi^i) \tag{56}$$

The error matrix E is

$$E = D + V\frac{1}{D}H \tag{57}$$

This implies

$$(\psi^i - \psi) = (A)^i(\psi^0 - \psi) \tag{58}$$

where the annihilation matrix A is

$$A = \frac{1}{V + H + E} E \tag{59}$$

This procedure converges if $\| A \| \leqslant 1$. This is so for any negative constant D for the case of Laplace's equation in a rectangle, and in fact the scheme is observed to converge for negative D in this case of the Grad-Shafranov equation on a torus.

The discussion to follow will consist of more or less heuristic considerations governing the choice of $D(j)$. We repeat for emphasis that the answer obtained by the iterative ADI scheme is independent of D. The convergence properties, however, do depend on D. An ill-advised choice will lead to poor convergence or even to no convergence. Setting D to zero, for example, produces a divergent series of approximants ψ^i, as can be seen by inspection of the error matrix E, Eq. (57).

The approximations to follow are used only to suggest appropriate D's; the equations the code solves are as given above.

We have used several choices for D. One is to set D roughly equal to $\sqrt{VH}$, by taking

$$D = -\frac{b}{r}\left\langle \frac{1}{rh_ih_j} \right\rangle = D(j) \tag{60}$$

where b is a numerical factor of order 1 chosen to optimize convergence. This value of D is used in the calculation of the initial equilibrium. To derive another choice, observe that an increase of ψ on one grid line j, implies a contraction of the volume of the plasma inside the flux surface labelled by the original value of ψ. This then will change P' and f' since the transport (conservation) equations depend on this volume To estimate the amount of feedback generated by this, integrate the toroidal flux Eq. (24), over ψ. Let ϕ be the toroidal flux contained inside flux surface ψ:

$$\phi = \int f \left\langle \frac{1}{r^2} \right\rangle V' \, d\psi \tag{61}$$

Then Eq. (24) becomes:

$$\frac{D\phi}{Dt} + c\langle \mathbf{E} \cdot \mathbf{B} \rangle V' = 0 \tag{62}$$

Now f is reasonably constant in a tokamak, where $\mathbf{B}_\varphi$ is almost entirely due to external windings. $\langle 1/r^2 \rangle$ does not have much variation either, being about $1/R^2$, where R is the major radius. Thus we can, roughly, set

$$\phi \cong \frac{f}{R^2} \int V' \, d\psi = \frac{f}{R^2} V(\psi) \tag{63}$$

Also, we have from Eqs. (34) and (44a):

$$c\langle E \cdot B \rangle = -\frac{\eta c^2}{4\pi} f \left(4\pi P' + ff' \left\langle \frac{1}{r^2} \right\rangle \right) \tag{64}$$

so

$$\frac{dV}{dt} \cong \frac{\eta c^2}{4\pi} R^2 V' \left(4\pi P' + ff' \left\langle \frac{1}{r^2} \right\rangle\right) \tag{65}$$

Since

$$\delta V(\psi) = -V' \delta\psi \tag{66}$$

we have

$$\delta\psi \cong -\Delta t \frac{\eta c^2}{4\pi} R^2 \delta \left(4\pi P' + ff' \left\langle \frac{1}{r^2} \right\rangle\right) \tag{67}$$

We now see that if the value of ψ on a j-line changes by an amount $\delta\psi$ there will be a resulting change in $4\pi P' + \langle ff'/r^2 \rangle$ as a result of the conservation laws. Let ψ^n be the value assumed for ψ on the j-line and used to calculate P and f. Then

$$\nabla \cdot \frac{1}{r^2} \nabla\psi + \left(4\pi P' + \frac{ff'}{r^2}\right)_{ij} - \frac{1}{(\eta c^2/4\pi)\, \Delta t\, R^2} (\psi - \psi^n) = 0 \tag{68}$$

is the proper equation. This gives

$$D = -\frac{1}{(\eta c^2/4\pi)\, \Delta t\, R^2} \tag{69}$$

In practice this is too large a damping factor, and the code requires many iterations per timestep. This is because this function successfully corrects for those errors which have ψ_{ij} too large (or small) for all i, but overestimates the effect on $4\pi P' + ff'/r^2$ of higher mode errors. It suffices to use a damping factor of, say .01 times that of Eq. (69). Notice that this D is inversely proportional to the timestep, whereas that given by

[redacted]

Shafranov equation. We now turn our attention to the numerical solution of the 1D conservation equations, (21)-(24).

Integrate these equations over ψ to find a form suitable for differencing. In general, for any function $a(\psi, t)$,

$$\frac{d}{dt} \int_{\psi_l(t)}^{\psi_u(t)} a(\psi', t)\, d\psi' = \int_{\psi_l(t)}^{\psi_u(t)} \frac{\partial a}{\partial t}\, d\psi + a(\psi_u, t) \frac{d\psi_u}{dt} - a(\psi_l, t) \frac{d\psi_l}{dt} \tag{70}$$

We will substitute for a the quantities nV', $\frac{3}{2}P_e V'$, $\frac{3}{2}P_i V'$, and $f\langle 1/r^2 \rangle V'$, in turn, to obtain integral forms of the conservation laws. The lower (ψ_l) and upper (ψ_u) bounds of the region of integration will in general be constant in time.

There are two regions, however, for which this is not so: the innermost and the outermost ones. The lower limit of integration of the innermost region is the value of ψ at the magnetic axis, a function of time. The upper limit of the outermost region is the value of ψ at the plasma boundary, determined by the specification of total plasma current as discussed above.

The effect of the $d\psi/dt$ terms is to convert the fluxes to those measured on a fixed grid, at the appropriate boundary. We take advantage of this at the origin, where the fluxes then vanish. At the outer boundary we retain $d\psi/dt$ explicitly in order to use the fluxes in the moving frame; these fluxes have the attractive feature that they vanish in the absence of collisions.

We label the flux surfaces by j; the magnetic axis is $j = 1$ and the outer boundary is $j = jm$. The conservation laws apply to the volume $\Delta V_{j+\frac{1}{2}}$ between surfaces j and $j+1$, the physical quantities are also defined at $j+\frac{1}{2}$. Their fluxes ($\boldsymbol{\Gamma}$, etc.) are defined on the j surfaces. The resulting difference equations are:

a) the innermost set, $j = 1$

$$\left(\frac{dn\,\Delta V}{dt}\right)_{\frac{3}{2}} + \langle \boldsymbol{\Gamma}_c \cdot \nabla V\rangle_2 = (\langle S\rangle\,\Delta V)_{\frac{3}{2}} \tag{71}$$

$$\frac{3}{2}\left(\frac{dP_e\,\Delta V}{dt}\right)_{\frac{3}{2}} + \left(P_e\frac{d\Delta V}{dt}\right)_{\frac{3}{2}} + \left\langle\left(\mathbf{Q}_e + \frac{5}{2}kT_e\boldsymbol{\Gamma}\right)\cdot\nabla V\right\rangle_2 = \left(\left\langle -\frac{c}{4\pi}f'\mathbf{E}\cdot\mathbf{B} - Q_\Delta + R_e\right\rangle\Delta V\right)_{\frac{3}{2}} \tag{72}$$

$$\frac{3}{2}\left(\frac{dP_i\,\Delta V}{dt}\right)_{\frac{3}{2}} + \left(P_i\frac{d\Delta V}{dt}\right)_{\frac{3}{2}} + \left\langle\left(\mathbf{Q}_i + \frac{5}{2}kT_i/\bar{z}\boldsymbol{\Gamma}_c\right)\cdot\nabla V\right\rangle_2 = (\langle Q_\Delta + R_i\rangle\,\Delta V)_{\frac{3}{2}} \tag{73}$$

$$\left(\frac{df\left\langle\frac{1}{r^2}\right\rangle\Delta V}{dt}\right)_{\frac{3}{2}} + \langle cV'\mathbf{E}\cdot\mathbf{B}\rangle_2 = 0 \tag{74}$$

b) the general set, $j = 2$ to $jm - 2$

$$\left(\frac{dn\,\Delta V}{dt}\right)_{j+\frac{1}{2}} + \langle \boldsymbol{\Gamma}_c\cdot\nabla V\rangle_{j+1} - \langle \boldsymbol{\Gamma}_c\cdot\nabla V\rangle_j = (\langle S\rangle\,\Delta V)_{j+\frac{1}{2}} \tag{75}$$

$$\frac{3}{2}\left(\frac{dP_e\,\Delta V}{dt}\right)_{j+\frac{1}{2}} + \left(P_e\frac{d\Delta V}{dt}\right)_{j+\frac{1}{2}} + \left\langle\left(\mathbf{Q}_e + \frac{5}{2}kT_e\boldsymbol{\Gamma}_c\right)\cdot\nabla V\right\rangle_{j+1} - \left\langle\left(\mathbf{Q}_e + \frac{5}{2}kT_e\boldsymbol{\Gamma}_c\right)\cdot\nabla\mathbf{V}\right\rangle_j = \left(\left\langle\frac{-c}{4\pi}f'\mathbf{E}\cdot\mathbf{B} - Q_\Delta + R_e\right\rangle\Delta V\right)_{j+\frac{1}{2}} \tag{76}$$

$$\frac{3}{2}\left(\frac{dP_i\,\Delta V}{dt}\right)_{j+\frac{1}{2}} + \left(P_i\frac{d\Delta V}{dt}\right)_{j+\frac{1}{2}} + \left\langle\left(Q_i + \frac{5}{2}kT_i/\bar{z}\boldsymbol{\Gamma}_c\right)\cdot\nabla V\right\rangle_{j+1} - \left\langle\left(\mathbf{Q}_i + \frac{5}{2}kT_i/\bar{z}\boldsymbol{\Gamma}_c\right)\cdot\nabla V\right\rangle_j = (\langle Q_\Delta + R_i\rangle\,\Delta V)_{j+\frac{1}{2}} \tag{77}$$

$$\left(\frac{df\left\langle\frac{1}{r^2}\right\rangle\Delta V}{dt}\right)_{j+\frac{1}{2}} + \langle cV'\mathbf{E}\cdot\mathbf{B}\rangle_{j+1} - \langle cV'\mathbf{E}\cdot\mathbf{B}\rangle_j = 0 \tag{78}$$

c) the outermost set, $j = jm - 1$

$$\left(\frac{dn\,\Delta V}{dt}\right)_{jm-\frac{1}{2}} + \langle \boldsymbol{\Gamma}_c \cdot \nabla V\rangle_{jm} - \langle \boldsymbol{\Gamma}_c \cdot \nabla V\rangle_{jm-1} = (\langle S\rangle\,\Delta V)_{jm-\frac{1}{2}} + (nV')_{jm}\frac{d\psi_{jm}}{dt} \tag{79}$$

$$\frac{3}{2}\left(\frac{dP_e\,\Delta V}{dt}\right)_{jm-\frac{1}{2}} + \left(P_e\frac{d\Delta V}{dt}\right)_{jm-\frac{1}{2}} + \left\langle\left(\mathbf{Q}_e + \frac{5}{2}kT_e\boldsymbol{\Gamma}_c\right)\cdot\nabla V\right\rangle_{jm} - \left\langle\left(\mathbf{Q}_e + \frac{5}{2}kT_e\boldsymbol{\Gamma}_c\right)\cdot\nabla V\right\rangle_{jm-1} = \left(\left\langle\frac{-c}{4\pi}f'\mathbf{E}\cdot\mathbf{B} - Q_\Delta + R_e\right\rangle\Delta V\right)_{jm-\frac{1}{2}} + \frac{5}{2}(P_eV')_{jm}\frac{d\psi_{jm}}{dt} \tag{80}$$

$$\frac{3}{2}\left(\frac{dP_i\,\Delta V}{dt}\right)_{jm-\frac{1}{2}} + \left(P_i\frac{d\Delta V}{dt}\right)_{jm-\frac{1}{2}} + \left\langle\left(\mathbf{Q}_i + \frac{5}{2}kT_i/\bar{z}\boldsymbol{\Gamma}_c\right)\cdot\nabla V\right\rangle_{jm} - \left\langle\left(\mathbf{Q}_i + \frac{5}{2}kT_i/\bar{z}\boldsymbol{\Gamma}_c\right)\cdot\nabla V\right\rangle_{jm-1} = (\langle Q_\Delta + R_i\rangle\,\Delta V)_{jm-\frac{1}{2}} + \frac{5}{2}(P_iV')_{jm}\frac{d\psi_{jm}}{dt} \tag{81}$$

$$\left(\frac{df\left\langle\frac{1}{r^2}\right\rangle\Delta V}{dt}\right)_{jm-\frac{1}{2}} + \langle cV'\mathbf{E}\cdot\mathbf{B}\rangle_{jm} - \langle cV'\mathbf{E}\cdot\mathbf{B}\rangle_{jm-1} = \left(f\left\langle\frac{1}{r^2}\right\rangle V'\right)_{jm}\frac{d\psi_{jm}}{dt} \tag{82}$$

These difference equations reduce to a 4×4 block tridiagonal set when the derivatives appearing the fluxes, Eqs. (29)–(31), (34), (44), are replaced by their difference analogues. We use the fully implicit "backwards" time centering for these equations, so their solution requires the inversion of a block tridiagonal matrix.

From time to time the innermost cell becomes too small in comparison with the others. When this happens, this cell is combined with the next one, the number of cells in the problem decreasing by one. Conversely, the growth of the outermost cell requires that it occasionally be split into two cells, the total number of cells thus increasing.

The method of solution of the 2D equation and the 1D set of equations has been described. The equations are coupled implicitly. In particular, the 1D set requires knowledge of $V(\psi, t)$, determined by the solution of the 2D equation. The 2D equation, in turn, requires knowledge of P and f, which are advanced in time by the 1D set. In order to solve both the sets simultaneously we use a subsidiary calculation for V, explicitly displaying its time dependence.

To obtain this equation, combine the flux surface average equations representing Faraday's law (24), Ohm's law (34), and Ampere's law (43). We find

$$\frac{D}{Dt}\left(f\left\langle\frac{1}{r^2}\right\rangle V'\right) + \frac{\partial}{\partial\psi}\eta_\parallel cf^2\frac{\partial}{\partial\psi}\frac{1}{f}\frac{K}{V'} = 0 \tag{83}$$

K and $\langle 1/r^2\rangle$ may be regarded as functions of V, changing in time only because the

shape of the flux surface containing volume V changes. We will assume that the shapes change slowly. K and $\langle 1/r^2 \rangle$, being integrals over the surface, change even more slowly. The function f is also relatively slowly changing, since in tokamaks f is primarily due to the external windings with steady currents. The resistivity $\eta_\parallel$ is assumed known.

If f, $\langle 1/r^2 \rangle$, and K are known functions, Eq. (83) tells us dV'/dt in terms of derivatives of V'. The boundary conditions are that K vanishes at the magnetic axis, which follows from its geometric definition, Eq. (41), and that at the wall

$$\left.\frac{K}{V'}\right|_W = \frac{4\pi}{c} I \tag{84}$$

where I is the toroidal current contained in the plasma, which follows from Eq. (45).

We need to specify the range of integration of Eq. (83) in ψ space. At the magnetic axis **E** and **B** both have only φ components, so Eqs. (10), (34), and (45) combine to give an equation for $d\psi/dt$ at the origin:

$$\dot{\psi}_0 = \eta_\parallel \frac{c^2}{4\pi} r^2 \frac{\partial \dfrac{K}{V'}}{\partial V} \tag{85}$$

The volume contained within the flux surface ψ satisfies

$$V(\psi) = \int_{\psi_0}^{\psi} V'(\tilde{\psi})\, d\tilde{\psi} \tag{86}$$

Since we have assumed we know the location of the outermost flux surface, we know the volume V_W contained. The value of ψ at the boundary, ψ_W, is therefore specified implicitly: it satisfies

$$V_W = \int_{\psi_0}^{\psi_W} V'(\tilde{\psi})\, d\tilde{\psi} \tag{87}$$

The numerical procedure for solving Eq. (83) is as follows. $V(\psi)$ is assumed known, therefore K and $\langle 1/r^2 \rangle$ are available as functions of ψ. The equation is linearized about the assumed $V(\psi)$, and represented by a tridiagonal difference equation for $\delta V(\psi)$, the deviation from the assumed V. ψ_W is found from the linearized solution, using Eq. (87). $V(\psi)$ is updated and the process repeated until δV becomes negligible.

These considerations suggest an algorithm for solving the 1D and 2D equations consistently. Replace D/Dt by its difference analogue, and begin an iterative scheme by assuming values for the functions f, $\langle 1/r^2 \rangle$, and K, namely those from the previous timestep.

Step A: With f, $\langle 1/r^2 \rangle$, and K known, Eq. (83) is the desired auxilliary equation specifying $V'(\psi, t)$ and ψ_W.

Step B: The solution of this equation gives the required information for the solution of the 1D set, Eqs. (75)-(78) and their end point forms, using Eqs. (29)-(31), and (44) for the transport terms.

Step C: The solution of these equations gives us P_e, P_i, and f at the new time. These functions specify the source terms for the 2D equation. The boundary value ψ_W is known from step A. The solution of this equation gives the shapes of the flux surfaces at the new time, and hence updated values of the shape-dependent functions $\langle 1/r^2 \rangle$ and K. Steps A, B, and C are repeated until the volume $V(\psi)$ calculated at C is sufficiently close to that calculated at step A.

VI. Examples

We will use as an example problem the calculation of the evolution of a large tokamak of elliptical outer cross section. The ellipse that defines the outer flux surface is centered 140 cm from the major axis, and is 45 by 45 $\sqrt{2}$ cm. The applied toroidal

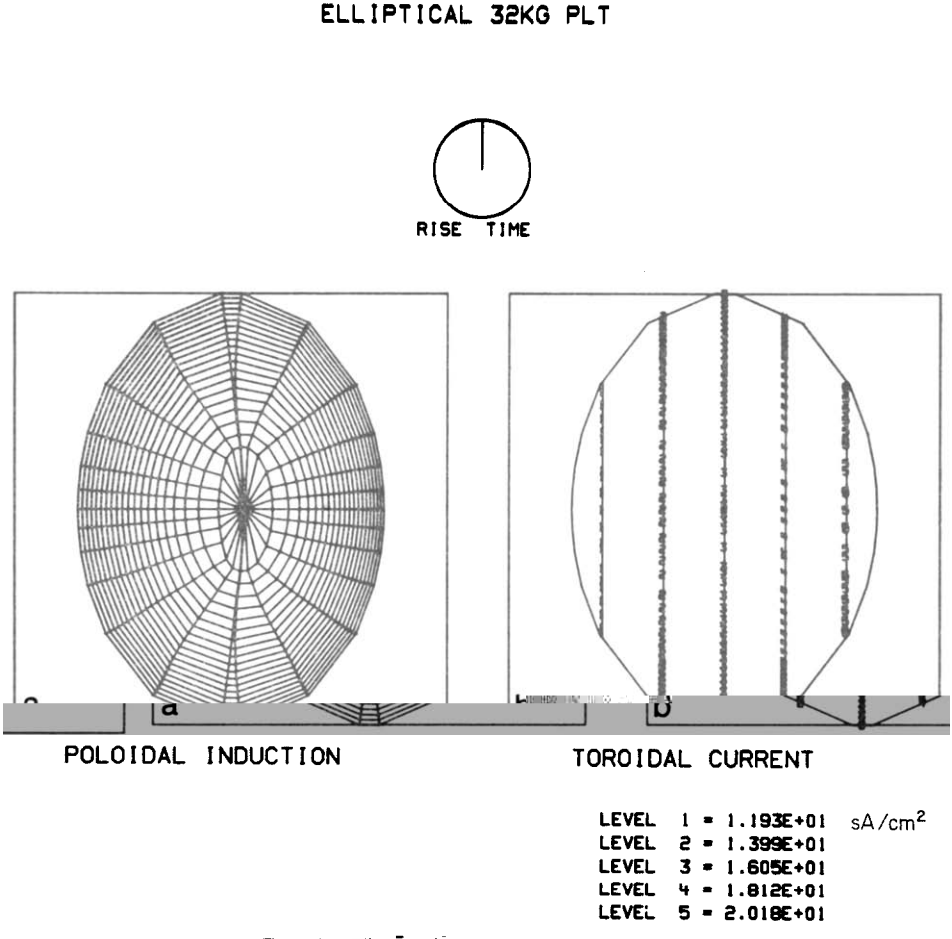

FIG. 4. Flux and current contours at $t = 0$.

field is 32 kG at 140 cm. The plasma has $\bar{z} = 1.6$ and $\bar{z}^2/\bar{z} = 4$. When the calculation begins the temperature of ions and of electrons is a uniform 50 eV, and the density increases almost parabolically from 4×10^{13} at the wall to 2×10^{14} at the center, with 145 kA of current. The current is distributed as a linear function of the distance r from the major radius. Figure 4a is a plot of the initial flux surfaces $\psi =$ constant, and Figure 4b is a plot of the initial current contours $j =$ constant, with higher numbers indicating higher current values. The axis of symmetry is on the left in these and subsequent plots.

The current is programmed to rise linearly in time to 600 kA at 0.1 seconds, then remain at that value. The calculation is carried out to 0.5 seconds. The wall temperatures are held at 50 eV, and the wall density at 4×10^{13}.

The first thing that one notices happening is that the current rapidly diffuses from its initial distribution towards uniformity. Figure 5a shows the flux surfaces and

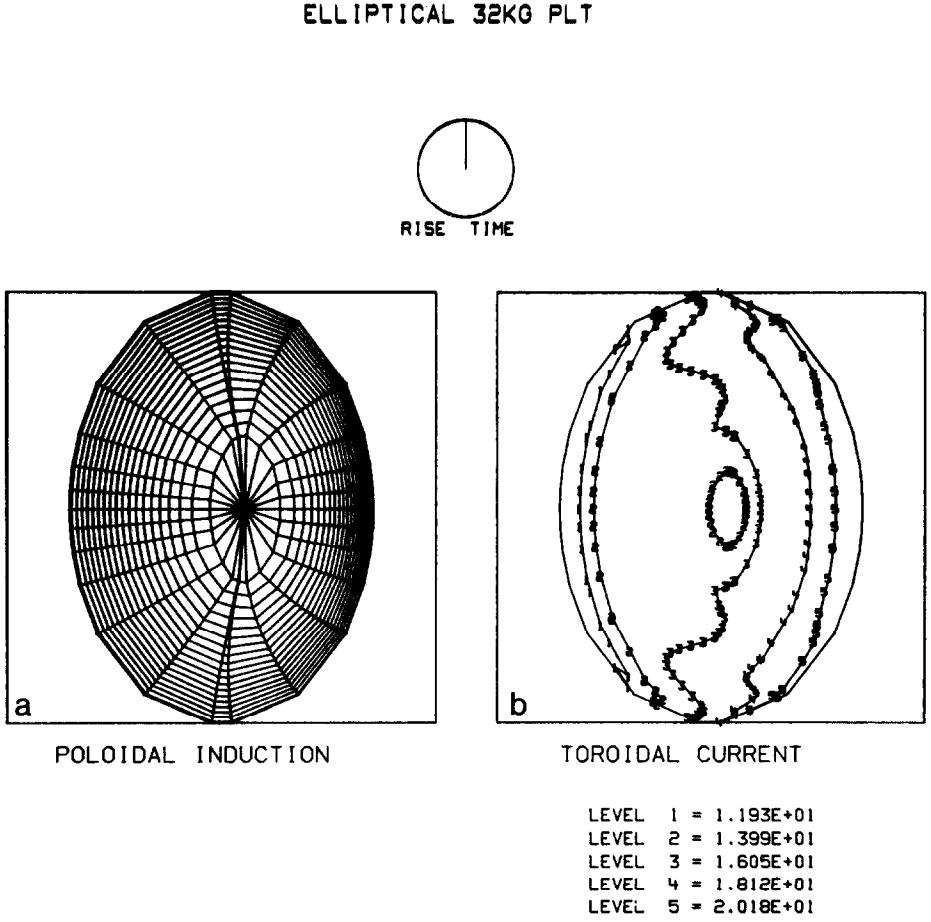

FIG. 5. Flux and current contours at $t = 3 \times 10^{-4}$.

Figure 5b the current contours at 10 cycles; problem time 3×10^{-4} sec. Figures 6a and 6b show the flux and current at 20 cycles, $t = 2.2 \times 10^{-3}$ seconds, when the total current is still only 154 kA and the central temperature is, at 52 eV, almost unchanged. The flux surfaces are almost unchanged, retaining their initial 7 cm off-center shift. (Of course, Ampere's law is satisfied, but the changes in j_φ are seen more easily than those in ψ since j_φ involves second derivatives.)

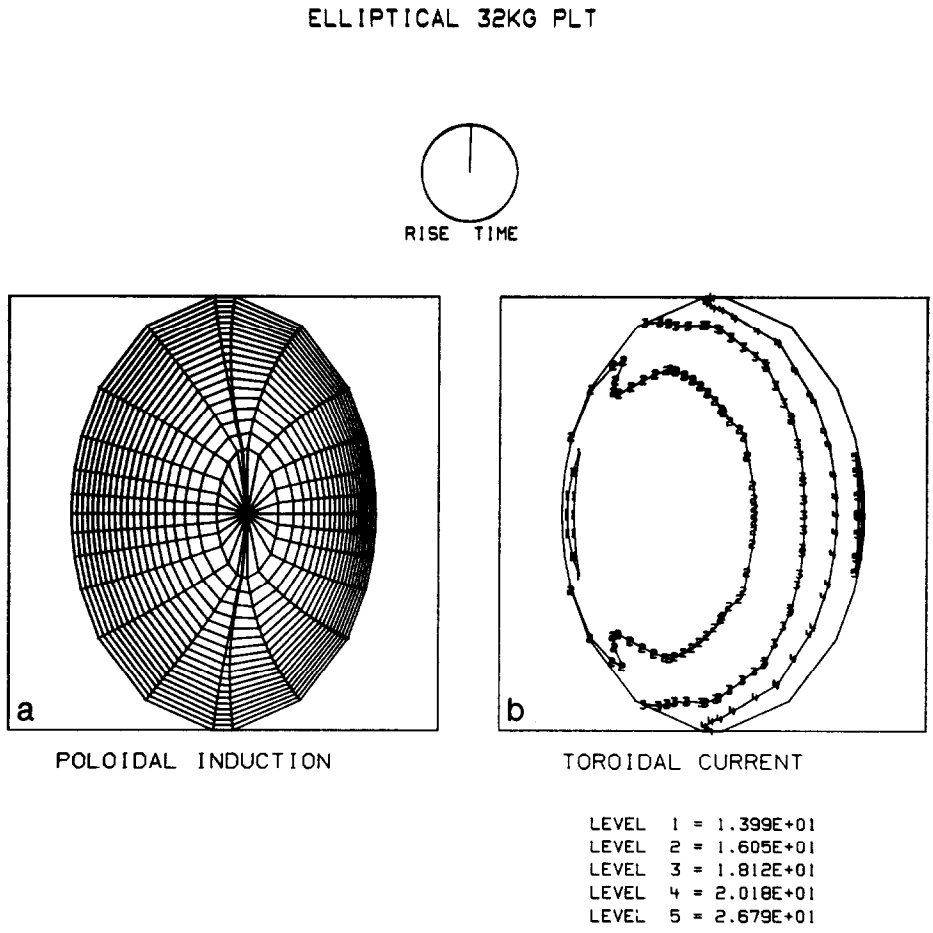

FIG. 6. Flux and current contours at $t = 2.2 \times 10^{-3}$.

The current continues to increase and the plasma to heat. At cycle 220, $t = .11$ seconds, the full 600 kA is in the plasma, and the central temperature has risen to 255 eV. The central density has dropped to 1.59×10^{14}, though the particle confinement time, $n/dn/dt$, for the whole tokamak is 2.1 seconds. Figures 7a and 7b show the flux surfaces and current at this time. Notice that the current is peaked

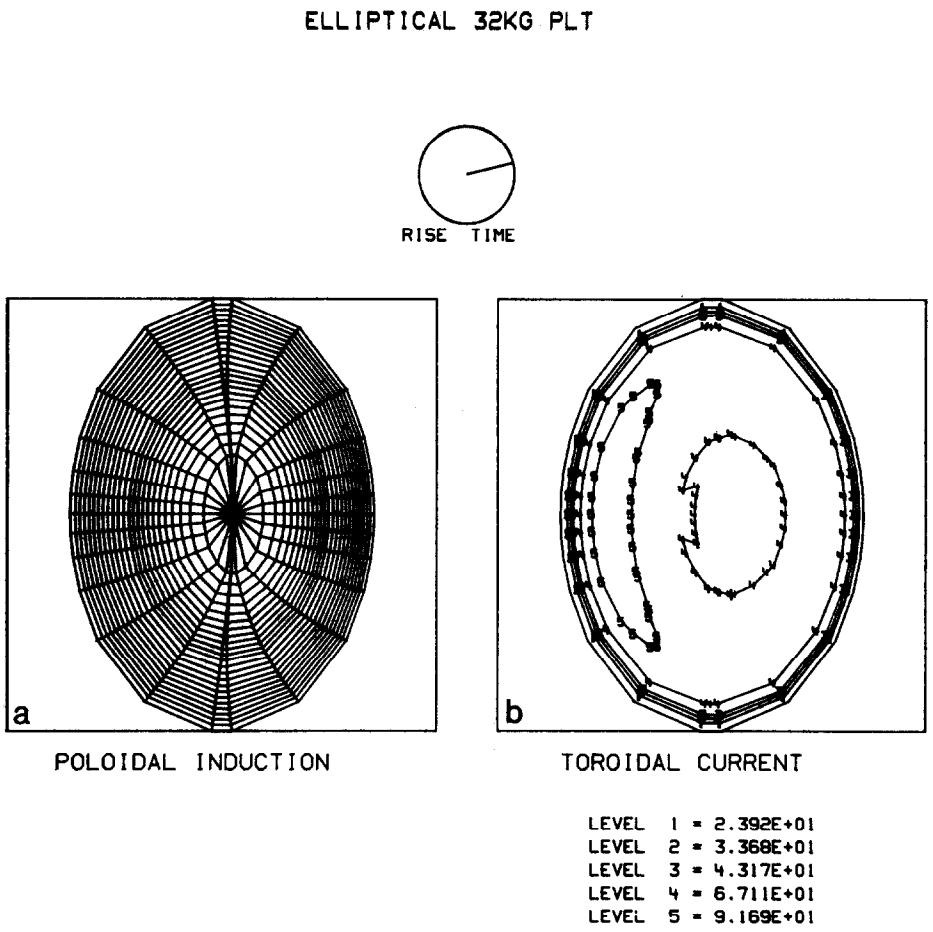

FIG. 7. Flux and current contours at $t = 0.11$.

toward the axis of the machine, and this has caused the flux surfaces to become more nearly centered; the off-center shift is now only 3 cm.

As the calculation proceeds the current tends to channel towards the center of the ellipse with the increase in the central temperature. At 0.5 seconds the contours of Figure 8a show the magnetic axis now 4.3 cm shifted, the flux surfaces tending toward circularity in the mid-regions, and the current peaked in the center. The safety factor q is 2.9 at the center, rising to 6.3 at the wall. The central density is 1.6×10^{14}, the temperature is 544 eV, and the energy confinement time is 75 msec. These results are of course strongly dependent on the fact that Pfirsch-Schlüter transport has been assumed. Other models, for instance trapped particle modes, give transport coefficients order of magnitude larger than those used in these runs and shorter confinement times.

Those results were obtained by using 26 poloidal zones (because of symmetry only

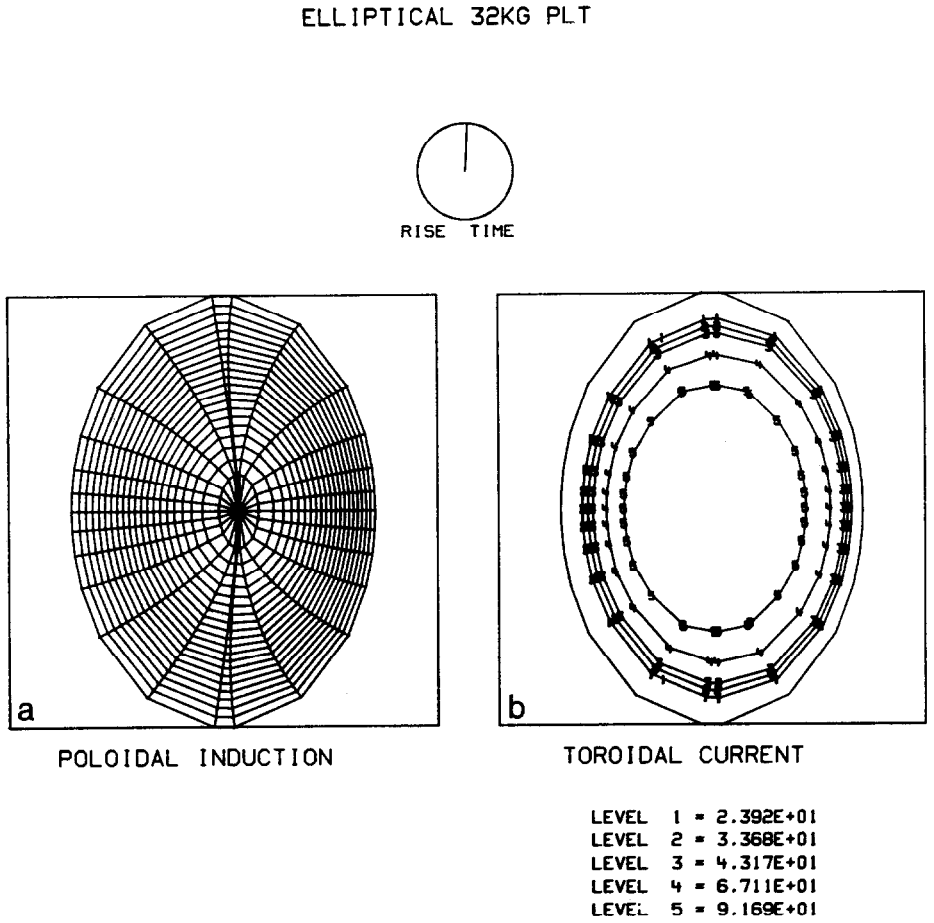

FIG. 8. Flux and current contours at $t = 0.5$.

13 are meaningful) and 21 radial (on the average, since the number can change). It is of interest to examine the sensitivity of the results to zoning. For this purpose we ran a series of four problems using the "1D" option discussed above: the geometry is given by tables which are calculated only once rather than being updated by the results of the 2D equilibrium solver. Another problem was run using 6, 11, 20 and 40 radial zones. The resulting histories of the central temperature are presented in Figure 9 for 6, 11 and 20 zones (the 40 zone case overlays the 20 zone case). It would appear 11 zones suffice for this problem, and in fact the plots of temperature vs. radius at 0.5 seconds, presented as Figure 10, show that the profiles, too, are reasonably well determined by 11 zones.

Finally, let us examine the necessity for a 2D code. The same problem was run in both 1D (static geometry) and 2D modes. Figure 11 plots temperature/time and Figure 12 temperature/radius at $\frac{1}{2}$ second. Figure 12 plots the temperatures from the

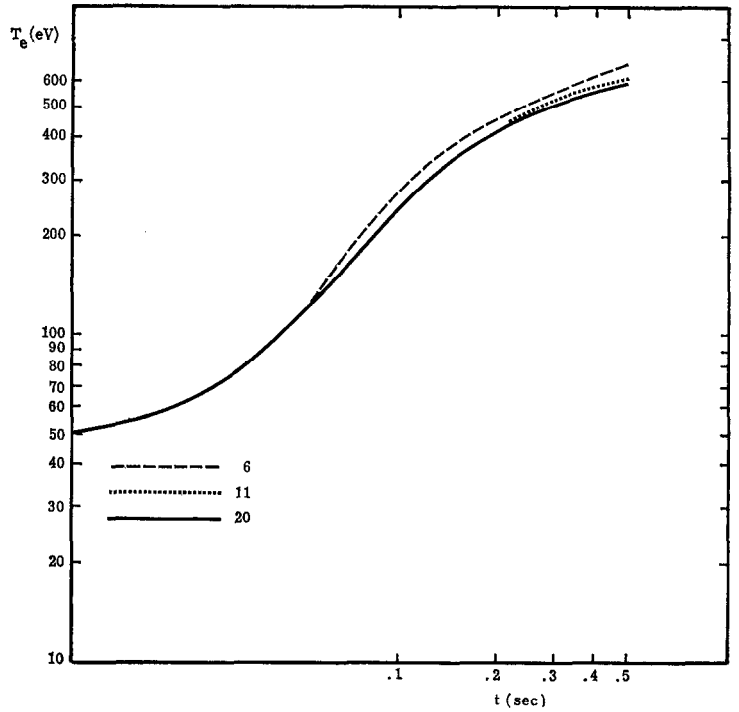

FIG. 9. Central temperature vs. time for various number of zones.

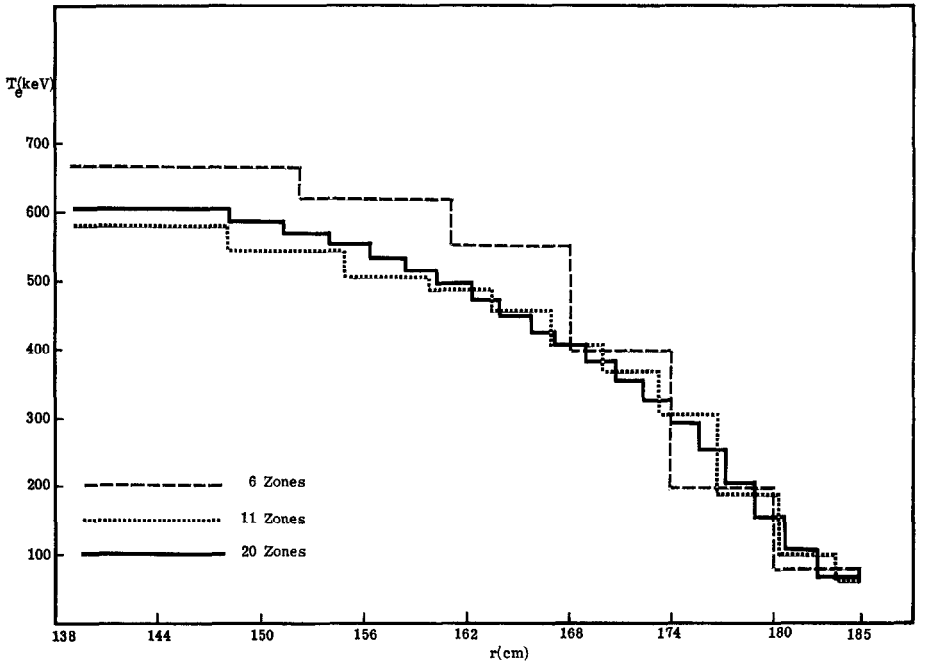

FIG. 10. Profiles at $t = .5$ for various number of zones.

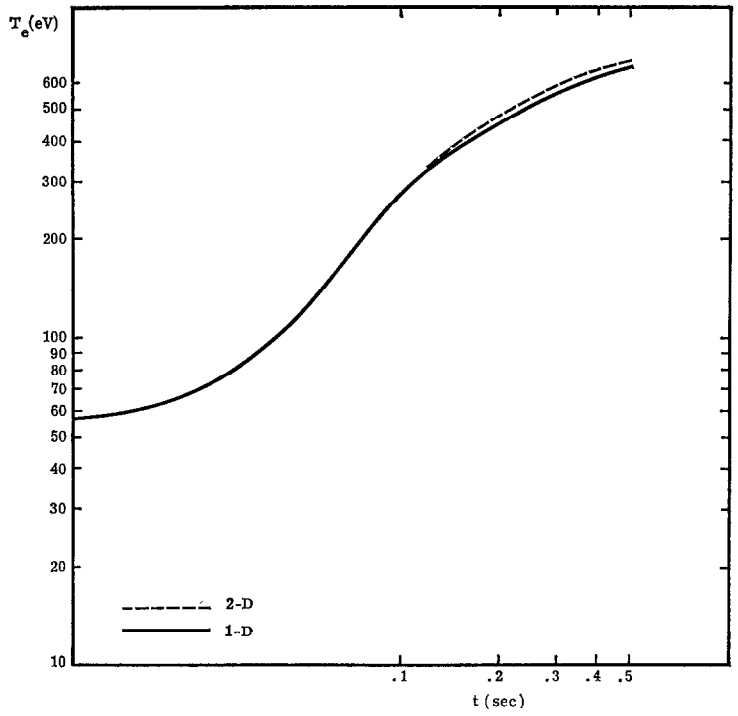

FIG. 11. Central temperatures vs. time, 1D and 2D.

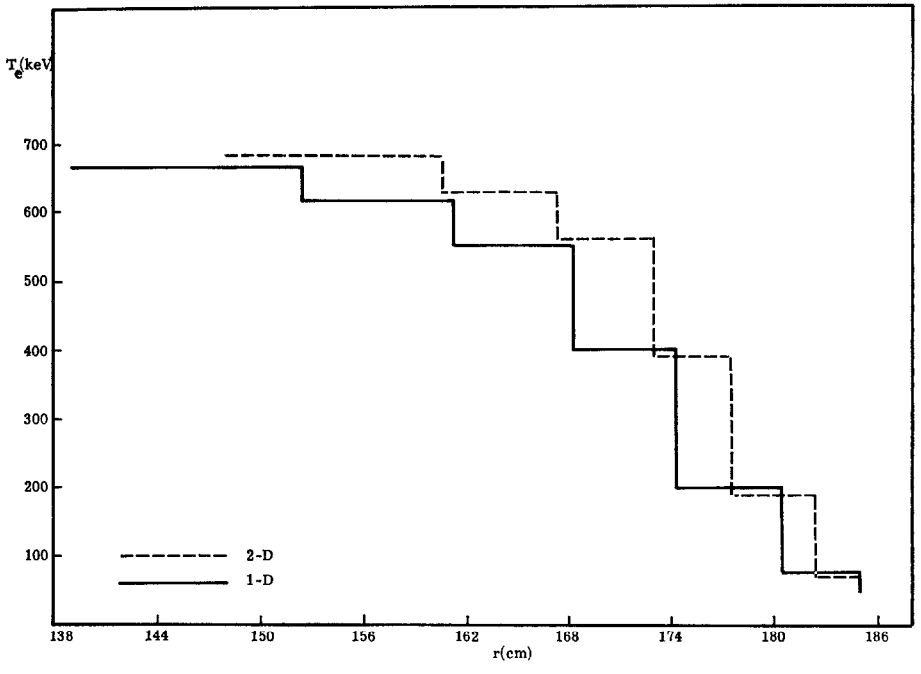

FIG. 12. Profiles at $t = .5$, 1D and 2D.

magnetic axis to the wall. It can be seen that a major difference between the 1D and the 2D results is the location of this axis, assumed to be in the geometric center for the 1D run. Its actual location was calculated in the 2D run.

VII. Conclusion

We have outlined and demonstrated a new technique for solving the transport equations in a coordinate system so that ψ remains constant on one coordinate. The transport is now that of Pfirsch and Schlüter, but the code can easily be modified to fit other regimes. The technique has proven to be both fast and accurate.

The G2M code is useful for modelling tokamaks for which a two dimensional description is required, such as those with a small aspect ratio or a noncircular cross section. The code is to our knowledge unique among existing 2D tokamak transport codes in that it calculates both toroidal and poloidal flux (from Faraday's law) and thus conserves both. Because of this the code will be a valuable tool in the investigation of the recently proposed "flux conserving" high beta tokamak [24].

APPENDIX A
Derivation of the 1D Conservation Laws

We will be interested in the time rate of change of flux surface integrals of some arbitrary quantity A. If $\mathbf{v}_\psi$ is the grid velocity, then the rules of differentiation tell us

$$\frac{d}{dt}\iiint_{\psi_l(t)}^{\psi_u(t)} A\, d^3X = \iiint_{\psi_l(t)}^{\psi_u(t)} (\dot{A} + \nabla \cdot A\mathbf{v}_\psi)\, d^3X \tag{A1}$$

We may do the surface integrals first, to find

$$\frac{d}{dt}\iiint_{\psi_l(t)}^{\psi_u(t)} A\, d^3X = \frac{d}{dt}\int_{\psi_l(t)}^{\psi_u(t)} \langle A\rangle\, V'\, d\hat{\psi} \tag{A2}$$

Since $\langle A\rangle V'$ are functions of ψ and t,

$$\frac{d}{dt}\int_{\psi_l(t)}^{\psi_u(t)} \langle A\rangle\, V'\, d\hat{\psi} = \int_{\psi_l(t)}^{\psi_u(t)} \frac{D\langle A\rangle\, V'}{Dt}\, d\hat{\psi} + \langle A\rangle\, V'\dot{\psi}\Big|_{\psi_u} - \langle A\rangle\, V'\dot{\psi}\Big|_{\psi_l} \tag{A3}$$

We may do the surface integrals on the right-hand side of Eq. A1

$$\frac{d}{dt}\iiint A\, d^3X = \int_{\psi_l}^{\psi_u} \left(\langle \dot{A}\rangle\, V' + \frac{\partial}{\partial\psi}\langle A\mathbf{v}_\psi \cdot \nabla V\rangle\right) d\hat{\psi} \tag{A4}$$

Combining,

$$\int_{\psi_l(t)}^{\psi_u(t)} \left(\frac{D\langle A\rangle V'}{Dt}\Big|_{\psi} - \langle \dot{A}\rangle V' - \frac{\partial}{\partial \psi}\langle A\mathbf{v}_{\psi}\cdot\nabla V\rangle \right) d\psi$$
$$+ \langle A\rangle V'\dot{\psi}\,|_u - \langle A\rangle V'\dot{\psi}\,|_l = 0 \tag{A5}$$

Since ψ_l and ψ_u are arbitrary, the integrand must vanish:

$$\frac{D\langle A\rangle V'}{Dt} = \langle \dot{A}\rangle V' + \frac{\partial}{\partial \psi}\langle A\mathbf{v}_{\psi}\cdot\nabla V\rangle \tag{A6}$$

Now substitute n for A:

$$\frac{DnV'}{Dt} = \langle \dot{n}\rangle V' + \frac{\partial}{\partial \psi}\langle n\mathbf{v}_{\psi}\cdot\nabla V\rangle \tag{A7}$$

Using Eq. (1) for n,

$$\frac{DnV'}{Dt} + \frac{\partial}{\partial \psi}\langle(\boldsymbol{\Gamma} - \boldsymbol{\Gamma}_G)\cdot\nabla V\rangle = \langle S\rangle V' \tag{A8}$$

The energy equations are only a bit more difficult to find. The terms in $\mathbf{Q}$, Q_{Δ}, and R are simple, as is the $\mathbf{E}\cdot\mathbf{B}$ part of $\mathbf{j}\cdot\mathbf{E}$, so consider the truncated equation

$$\frac{3}{2}\dot{P} + \frac{5}{2}\nabla\cdot kT\boldsymbol{\Gamma} = \mathbf{v}_{\psi}\cdot\nabla P \tag{A9}$$

We find from Eq. A6

$$\frac{3}{2}\frac{DPV'}{Dt} = \frac{3}{2}\langle\dot{P}\rangle V' + \frac{\partial}{\partial\psi}\left\langle\frac{3}{2}P\mathbf{v}_{\psi}\cdot\nabla V\right\rangle \tag{A10}$$

Using Eq. A9 for P

$$\frac{3}{2}\frac{DPV'}{Dt} = -V'\left\langle\frac{5}{2}\nabla\cdot kT\boldsymbol{\Gamma}\right\rangle + V'\langle\mathbf{v}_{\psi}\cdot\nabla P\rangle + \frac{\partial}{\partial\psi}\left\langle\frac{3}{2}P\mathbf{v}_{\psi}\cdot\nabla V\right\rangle \tag{A11}$$

Finally, from Eq. A6 for (DV'/Dt)

$$\frac{3}{2}\frac{DPV'}{Dt} = -\frac{5}{2}\frac{\partial}{\partial\psi}\langle kT\boldsymbol{\Gamma}_c\cdot\nabla V\rangle - P\frac{dV'}{dt} \tag{A12}$$

This is the desired result.

ACKNOWLEDGMENTS

We are pleased to acknowledge helpful discussions with Dr. N. A. Krall and Dr. D. Potter. One of us (R. N. B.) was a visitor at the Courant Institute during the preparation of the manuscript and gratefully acknowledges the hospitality of Professor H. Grad. We owe our understanding of the function $K(V)$ and its role in the code to Professor Grad. We are indebted to Ms. Sonya Wier for her expert typing of a difficult manuscript.

This work was supported by the United States Energy Research and Development Administration under Contract AT-(04-3)-1018.

REFERENCES

1. F. L. RIBE, *Rev. Mod. Phys.* **47** (1975), 2.
2. L. A. ARTSIMOVICH, *Nucl. Fusion* **12** (1972), 215.
3. S. O. DEAN *et al.*, "Status and Objectives of Tokamak Systems for Fusion Research," E.R.D.A. Report WASH-1295, Superintendant of Documents, U.S. Government Printing Office, Washington, D. C., 1974.
4. H. P. FURTH, *Nucl. Fusion* **15**, 487 (1975).
5. C. CHU, K. MORTON, AND K. ROBERTS, "Proc. 3rd International Symposium on Numerical Fluid Dynamics (Paris, 1972)," Springer–Verlag, Berlin/New York, 1973.
6. H. GRAD AND J. HOGAN, *Phys. Rev. Lett.* **24**, 1337 (1971).
7. J. HOGAN, "Multifluid Tokamak Transport Models," Methods in Comp. Phys., Vol. 16, p. 131, Academic Press, New York/London, 1976.
8. H. GRAD, Oak Ridge National Laboratory memos of 22 April and 6 July, 1970.
9. F. HINTON AND R. HAZELTINE, *Rev. Mod. Phys.* **48** (1976), 239.
10. J. HELTON, R. MILLER, AND J. RAWLS, *Bull. Amer. Phys. Soc. II* **20** (10 Oct. 1975).
11. A. TODD AND R. GRIMM, *Bull. Amer. Phys. Soc. II* **20** (10 Oct. 1975).
12. J. GARDNER AND J. BORIS, "Proc. of Theo. Aspects of C.T.R.," unpublished, 1975.
13. R. HAZELTINE AND F. HINTON, *Phys. Fluids* **16**, 1883 (1973).
14. Y.-P. PAO, *Phys. Fluids* **19**, 1177 (1976).
15. H. GRAD AND H. RUBIN, *in* "Proc. 2nd Int'l. Conf. on Peaceful Uses of Atomic Energy," United Nations, Geneva, 1958.
16. V. SHAFRANOV, JETP **8**, 545 (1958).
17. L. SPITZER, "Physics of Fully Ionized Plasmas," Interscience, New York/London, 1967.
18. S. I. BRAGINSKII, "Transport Processes in Plasmas," Reviews of Plasma Physics, Vol. 1, p. 205, Consultants Bureau, New York, 1965.
19. H. GRAD, P. HU, AND D. STEVENS, *Proc. Nat. Acad. Sci. USA* **72**, 3789 (1975).
20. D. POTTER, "Waterbag Methods in Magnetohydrodynamics," Methods in Comp. Phys., Vol. 16, p. 43, Academic Press, Vol. 16, 0. 43, 1976.
21. G. TUTTLE, D. POTTER, AND G. HAINES, "Proc. 5th Conf. on Plasma Physics and Controlled Nuclear Fusion Research, Tokyo," IAEA-CN-33, 1974.
22. D. POTTER AND G. TUTTLE, *J. Comp. Phys.* **13** (1973), 483.
23. G. BIRKHOFF, "Numerical Solution of Elliptic Equations," SIAM, 1971.
24. J. CLARKE, *Bull. Amer. Phys. Soc.* **20**, 1228 (1975).